
Performance analysis of GO gel composite coating on electro-spark deposited surfaces

Xin Du

«Xinxiang University», Xinxiang, China

Faculty of Engineering Technology «Sumy National Agrarian University», Sumy, Ukraine

ORCID 0000-0002-1996-602X

Viacheslav Tarelnyk

Faculty of Engineering Technology «Sumy National Agrarian University», Sumy, Ukraine

ORCID 0000-0003-2005-5861

To cite this article:

Du Xin, Tarelnyk Viacheslav. Performance analysis of GO gel composite coating on electro-spark deposited surfaces. International Science Journal of Engineering & Agriculture. Vol. 2, No. 5, 2023, pp. 20-30. doi: 10.46299/j.isjea.20230205.03.

Received: 09 13, 2023; **Accepted:** 09 29, 2023; **Published:** 10 01, 2023

Abstract: The uneven surface roughness observed in the electro-spark deposition (ESD) process can be attributed to the unsteady pulsed electrical energy. ESD coating frequently needs to be processed in order to achieve higher surface quality. The surface of the coating undergoes processing techniques such as grinding, ultrasonic processing, and rolling. Because some coatings are hard and the surface hardness is uneven, surface processing is complicated. When a grinder is used for processing, the coating thickness is not easy to control. The product performance is uneven. When non-metallic coatings are used, it can enhance the surface quality of the coating. This study used a composite coating of sodium silicate and lubricating particles. Three coating schemes were studied. Graphene oxide (GO) gel and sodium silicate composite coating have the best overall performance. It can effectively improve the surface quality of the coating, with less roughness and better wear resistance. Graphene oxide gel is used to solve the problem of lubricating particle agglomeration. When it was actually applied to the SKH51 layer, the surface roughness Ra was reduced from 1.086 μm to 0.113 μm . It is effective in reducing friction and wear.

Keywords: GO gel, Composite coating, Raman analysis, Abrasion resistance, Friction coefficient, Surface morphology.

1. Introduction

The electro-spark deposition (ESD) method of pulse energy cannot proceed continuously, which results in a significant amount of surface roughness being deposited. Machine processing can improve the surface accuracy of ESD. The coating surface can be processed by grinding, ultrasonic processing, rolling and other methods. These methods can improve the surface quality of ESD coatings. These methods add complexity and cost to the surface modification process.

Improving surface quality has become an industry challenge for electro-spark deposition. Traditionally, grinding machines are utilised for processing. The coating thickness is not easy to control and the product performance is not uniform. The production efficiency of ultrasonic processing is even lower. Non-metallic coatings are used to reduce the roughness of the ESD surface and improve the ESD surface accuracy through an additive process. It reduces manufacturing costs and avoids scrap. Non-metallic coatings can significantly reduce surface roughness and have certain

abrasion resistance. Lubricant particles are used to modify non-metallic coatings to improve the abrasion resistance of the coating.

2. Object and subject of research

The object of the research is non-metallic coating deposition process. The subject of the study is the comparison of three non-metallic coating schemes, which can improve the surface quality of ESD coating and improve the overall performance of the coating.

3. Target of research

The purpose of this study is to improve surface quality and performance of ESD coatings. This research uses additive processing to replace the traditional method of subtractive processing to reduce processing costs and improve yield rate.

To achieve the goal, it is necessary to: Choose a non-metallic paint that creates a harder coating. It is necessary to reasonably select modified lubricating particles to improve the overall performance of the coating. These non-metallic coatings will be comprehensively analyzed in terms of material composition, surface morphology, surface roughness, friction coefficient, and wear scar width.

4. Literature analysis

Ribalko used low energy pulses to grind deposits and improve surface accuracy (Ribalko, Sahin, & Korkmaz, 2009). In order to improve the surface roughness, Gadalov uses VOK-60 mineral ceramics to polish the surface (Gadalov, Romanenko, Samoilov, Nikolaenko, & Grigor'ev, 2012). With lower discharge energy, Kirik improved the surface quality of aluminium coating surfaces and reduced the roughness (Kirik, Gaponova, Tarelynyk, Myslyvchenko, & Antoszewski, 2018). Enrique uses machine hammer grinding to reduce ESD surface roughness (Enrique et al., 2020). The polymer coating has a lower hardness than the metal coating, but the surface roughness is significantly reduced (Dovzhik, Tarelnik, Marcinkovsky, & Pavlov, 2016).

Because of its low cost and easy availability, graphene oxide (GO) was an excellent filler for non-metal nanocomposites (Ding et al., 2018; Smith, LaChance, Zeng, Liu, & Sun, 2019; Yu, Sisi, Haiyan, & Jie, 2020). Graphene oxide has the characteristics of low density, large specific surface area, high mechanical strength, high mechanical properties, and good wear resistance (Compton & Nguyen, 2010; Im & Kim, 2012; Tong et al., 2016; Wojtoniszak et al., 2012; Zhu et al., 2010). Due to this combination of properties, GO materials have extraordinary efficiency. GO has the structure of graphene and hydrophilicity that graphene does not have (Neklyudov, Khafizov, Sedov, & Dimiev, 2017; Yu et al., 2020). Graphene oxide dissolves in water and becomes a gelatinous solution when the content of GO increases (Yeh, Raidongia, Shao, Yang, & Huang, 2015). Graphene oxide dissolves in water and becomes a gelatinous aqueous solution when the GO content increases. In this way, it will avoid the flocculent agglomeration of graphite oxide. Graphite oxide has been used in coating studies (Ghauri, Raza, Baig, & Ibrahim, 2017; Krishnamoorthy et al., 2014; Kumar, Bashir, Ramesh, & Ramesh, 2021; Palmieri et al., 2016).

5. Research methods

The performance of three coatings was analyzed, which were GO gel composite coating, sodium silicate (Na_2SiO_3) coating, and composite coating of sodium silicate and graphite. And GO gel coating was coated on the SKH51 coating of electro-spark deposition for experimental comparison.

5.1 Preparation method for GO gel composite coating

Liquid sodium silicate solution was used, as shown in Table 1 (YOU RUI Refractory Material Co., Ltd., China). Industrial graphene oxide gel solutions were used at a concentration of 10mg/ml (Suzhou TANFENG grapheme Tech Co., Ltd, China). Liquid sodium silicate solution and graphene oxide gel solution were mixed in a 1:1 volume ratio. Next, mechanical-physical mixing was carried out for twenty minutes with a shaker. Then, the surface of the metal specimen was painted with a brush. After that, it was baked in a dry heating oven at 80°C for 2 hours and cooled in an oven for 1 hour. Coatings can often be re-coated and baked to obtain more number of layers and thicknesses.

Table 1. Sodium silicate liquid technical indexes

Type	Na ₂ O	SiO ₂	Density (20°C)	Baumé degrees	Solid content
SP38	8.53%	26.98%	1.366 g/cm ³	38.5°Bé	35.5%

5.2 Preparation of sodium silicate coating

Sodium silicate liquid solution was applied to the surface of the metal substrate as shown in Table 1 (YOU RUI Refractory Material Co., Ltd., China). Next, mechanical-physical mixing was carried out for twenty minutes with a shaker. Then, the surface of the metal specimen was painted with a brush. Then, it was baked in a dry heating oven to 80 for 2 hours and then cooled to room temperature in the oven.

5.3 Preparation of sodium silicate and graphite composite coatings

Graphite powder was used (Tianjin DENGKE Chemical Reagent co., LTD, China). Liquid sodium silicate solution and graphite powder were chosen to be mixed at a mass ratio of 10:1. It was packed in a specimen box. Mechanical-physical mixing was carried out for 20 minutes with a shaker. Then, the surface of the specimen was coated with a dropper. It was baked in a drying oven to 80°C and then cooled in the oven for 60 minutes. If more layers and thicknesses of coating were required, re-coating and baking were usually necessary.

5.4 Testing methods

The coatings were observed for the surface morphology of the coatings by a Leica super depth of field microscope (LEICA DVM6, Germany). GO gel composite coating and sodium silicate coatings were analyzed by laser Raman spectroscopy. Wear resistance analysis of the coating surfaces was carried out by linear reciprocating friction and wear machine (MWF-500, China). The width of the wear grooves was analyzed by super depth of field microscope.

6. Research results

6.1 Morphological analysis of GO gel composite coatings

Observations of the surface morphology were carried out by super depth of field microscope (LEICA DVM6), as shown in Fig. 1. In the 100X two-dimensional morphology, there are tiny bubbles on the surface of the Go gel composite coating, as shown in Fig.1. When the microscope was

magnified 500 times, it can be seen the graphene oxide particles and the traces of brush application, as in Fig.1. Through the 3D morphology synthesized by the depth of field of the microscope, it was found that the surface of the GO gel composite coating was relatively flat. The coating surface was smooth and has good gloss.

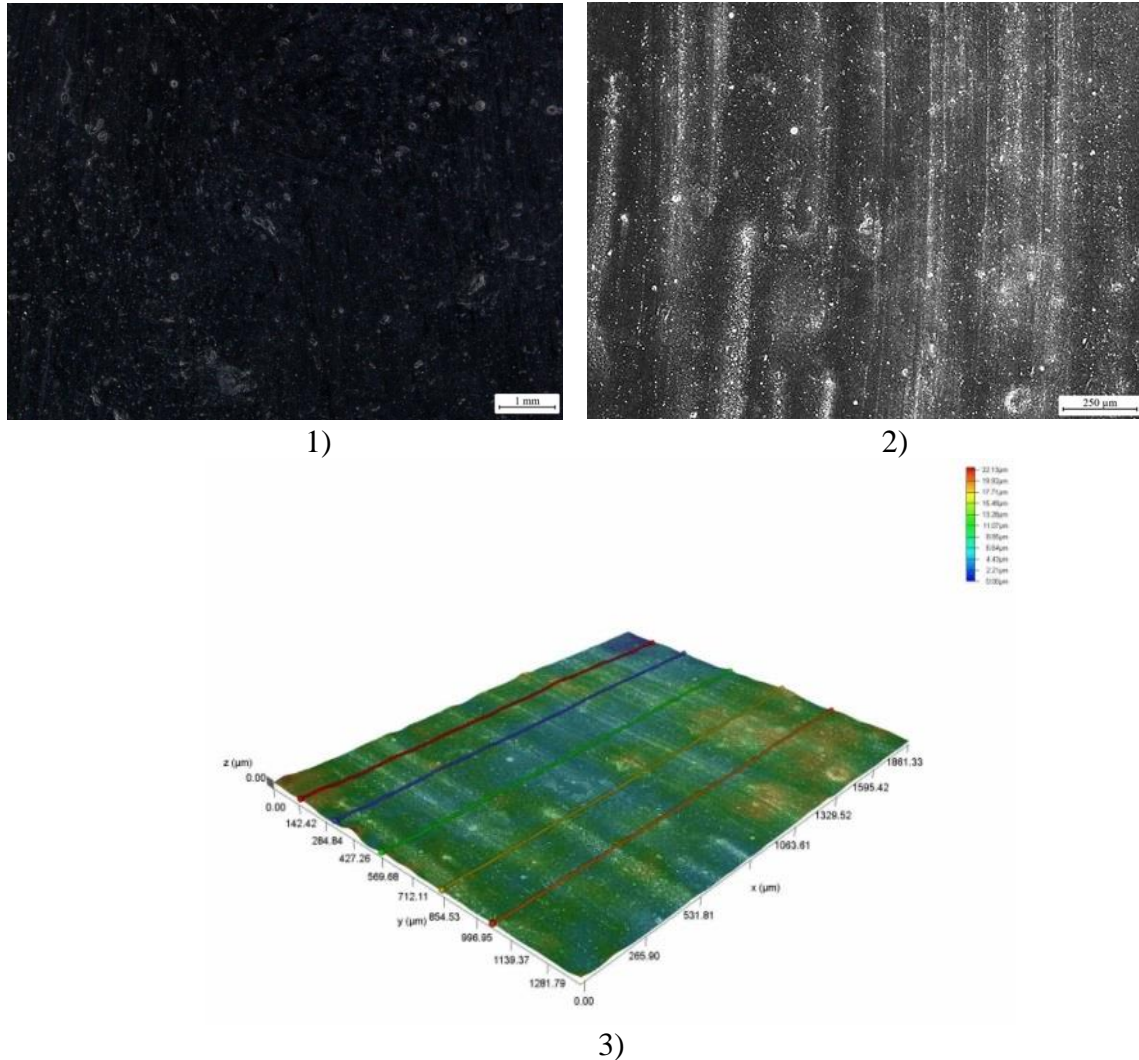


Fig. 1. Surface morphology of Go gel composite coating: 1-100X 2D morphology;2-500X 2D morphology; 3- super depth field of 3D morphology.

6.2 Raman spectrum detection

Laser Raman spectrum can analyze ions, molecular species and the structure of substances. This experiment used the DXR2xi instrument from Thermo Fisher company, the device parameters are shown in Table 2. Laser Raman is commonly used in the analysis of graphene oxide and graphene materials. This type of material has unique characteristics that are easily recognizable (Huang et al., 2013; Nakamizo, Kammereck, & Walker Jr, 1974).

Table 2. The parameters of thermo scientific DXR2xi

Type	Company	Laser	Spectrum range	Spectrum resolution
DXR2xi	Thermo Fisher	532nm	50cm ⁻¹ -6000cm ⁻¹	<1.5cm ⁻¹

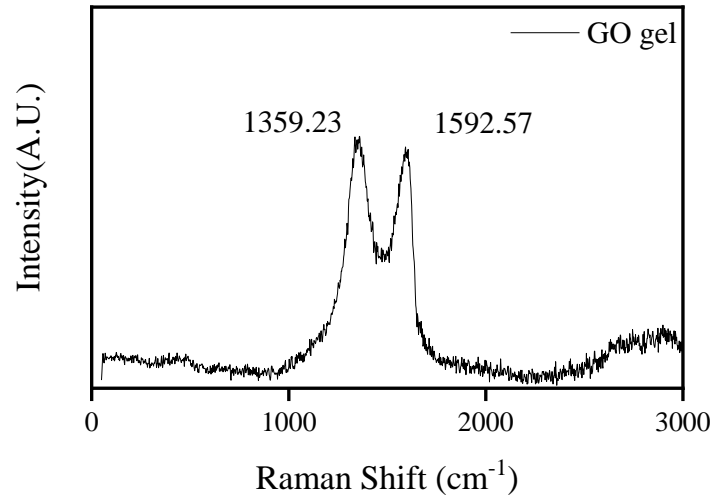


Fig. 2. Raman diagram of GO gel composite coating.

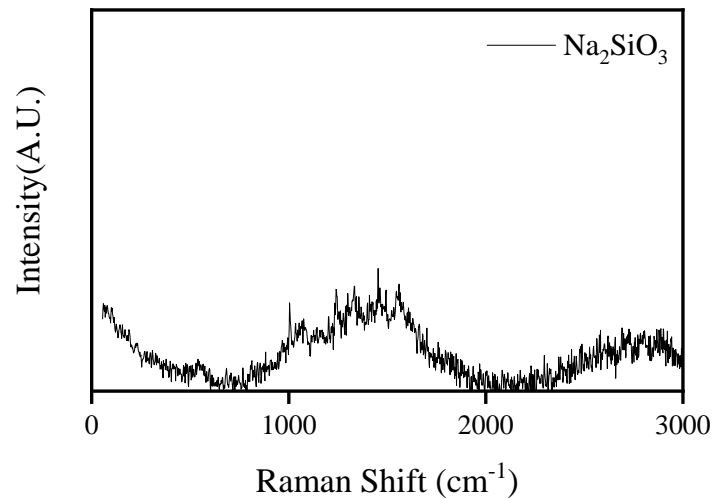


Fig. 3. Raman diagram of Na₂SiO₃ coating.

In the measured Raman spectrum (Fig. 2), it can be observed that there are two characteristic peaks located at 1359.23 cm^{-1} and 1592.57 cm^{-1} (Gao et al., 2021; Sun et al., 2019). Nano-carbon materials usually contain two obvious Raman peaks during research. It was found that the peak between 1359.23 cm^{-1} is the A1g vibration mode of the sp³ electronic structure of diamond-like carbon. The peak located between 1592.57 cm^{-1} is considered to be the E2g vibration mode of the sp² electronic structure of graphitic carbon.

In Fig. 3 is a Na₂SiO₃ coating without GO material, since its Raman pattern does not show two obvious characteristic peaks. Therefore, the two coatings contain different compositions from the Raman diagrams.

6.3 Surface roughness

Coating surface roughness can be measured with Mitutoyo SJ-210 roughness tester. When the surface roughness was measured, the experiment adopted the ISO 1997 standard, as shown in Table 3. Three surface measurements were performed on each sample to determine their surface roughness. It shows the average roughness of the coatings in Table 4. From Table 4, the sodium silicate (Na₂SiO₃) coating has the lowest roughness with a Ra value of $0.015\text{ }\mu\text{m}$. SKH51 deposited coating

has the highest roughness value with a Ra value of 1.086 μm . The surface roughness of the GO gel composite coating was 0.16 μm because of the effects of micro-bubbles and the brush coating process.

Na_2SiO_3 and graphite composite coating has a roughness of 0.454 μm as the size of graphite particles. When the GO gel composite coating was coated on the surface of SKH51, the roughness value decreased from 1.086 μm to 0.113 μm . Therefore, the Go gel composite coating can reduce the surface roughness of ESD coating.

Table 3. Mitutoyo SJ-210 roughness measurement parameters

Standard	Profile	λ_s	Evaluation Length	Cut-Off	Filter
ISO 1997	R	2.5 μm	2.92mm	0.08mm	GAUSS

Table 4. Surface roughness of coating

NO.	Na_2SiO_3 coating	GO gel composite coating	Na_2SiO_3 graphite Composite coating	SKH51 coating	SKH51+GO gel composite coating
1	0.013 μm	0.131 μm	0.373 μm	0.949 μm	0.077 μm
2	0.021 μm	0.153 μm	0.643 μm	1.095 μm	0.176 μm
3	0.011 μm	0.197 μm	0.347 μm	1.213 μm	0.087 μm
Average value	0.015 μm	0.160 μm	0.454 μm	1.086 μm	0.113 μm

6.4 Abrasion resistance analysis

1) Coefficient of friction

Abrasion resistance experiments were conducted on Go gel composite coating, Na_2SiO_3 coating, SKH51+Go gel composite coating, and Na_2SiO_3 graphite composite coating. The SKH51+go gel composite coating is selected on 45 steel sheets with a size of 25*30mm. The SKH51 material was coated on the surface of 45 steel by the ESD process, .The Go gel composite coating was coated on the SKH51 layer. The same heating process was used for surface of GO gel coating.

The abrasion resistance of surface coating was evaluated with the linear reciprocating abrasion machine MWF-500. The friction machine uses ZrO_2 friction balls with a size of 6mm and surface accuracy of G10 as the counter-grinding material. It was used a pressure of 30N in testing. The equipment motor has a speed of 100r/min, a reciprocating distance of 6mm, and the motor performs 2 movements per revolution. The test time is 10 minutes, and the surface dry friction test is carried out. The friction ball is replaced for each experiment and the surface is wiped with absolute ethanol. Dry friction experiments were conducted on four coatings, and the results are shown in Fig. 4. Since the surface of SKH51 has a certain roughness, the coefficient of friction of SKH51+GO gel composite coating is slightly larger than that of GO gel composite coating. It shows that the Na_2SiO_3 coating has the highest friction coefficient of 0.28, while the gel graphite coating has the lowest friction coefficient of 0.14, and the GO gel composite coating has the low friction coefficient of 0.17 in Table 5. The friction coefficient of GO gel composite coating is 39.2% lower than that of Na_2SiO_3 coating.

It is shown that the GO gel material can reduce the coefficient of friction and the friction force. The surface quality of the metal substrate will also affect the friction coefficient of the coating.

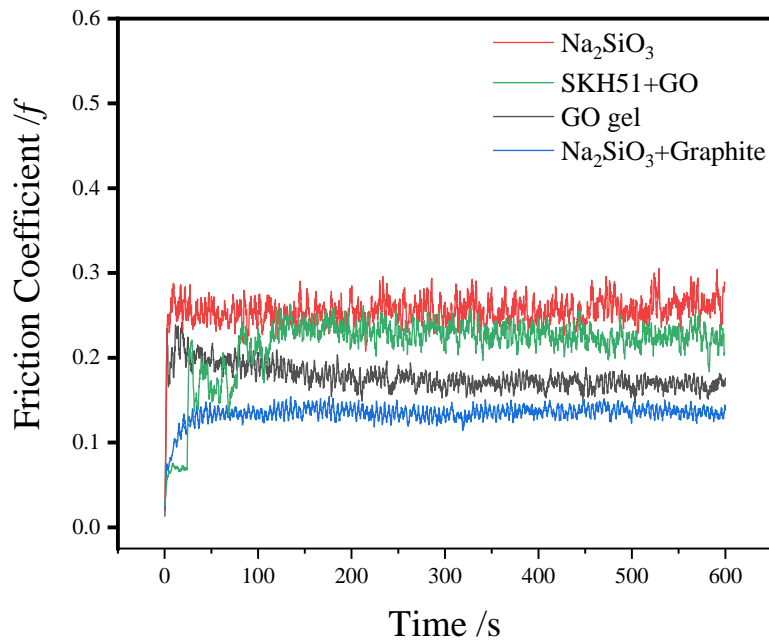


Fig. 4. Friction coefficient of non-metallic coatings.

Table 5. Average friction coefficient of coating

Type	Na ₂ SiO ₃ coating	GO gel Composite coating	Na ₂ SiO ₃ graphite composite coating	SKH51+GO gel composite coating
Average friction coefficient	0.28	0.17	0.14	0.20

2) Abrasion mark width

The maximum width of the abrasion marks was measured with an ultra-deep field microscope, as shown in Fig.5. (Jiang et al., 2021; Shi et al., 2022). Due to the effect of the roughness of the coating surface, the abrasion marks are not uniform and the friction force and coefficient of friction do not accurately reflect the degree of wear resistance. Therefore, the standard deviation of the maximum average width of the abrasion marks was applied to determine the quality of the abrasion marks. For each specimen, the average value of equally spaced abrasion marks was measured and the standard deviation was determined.

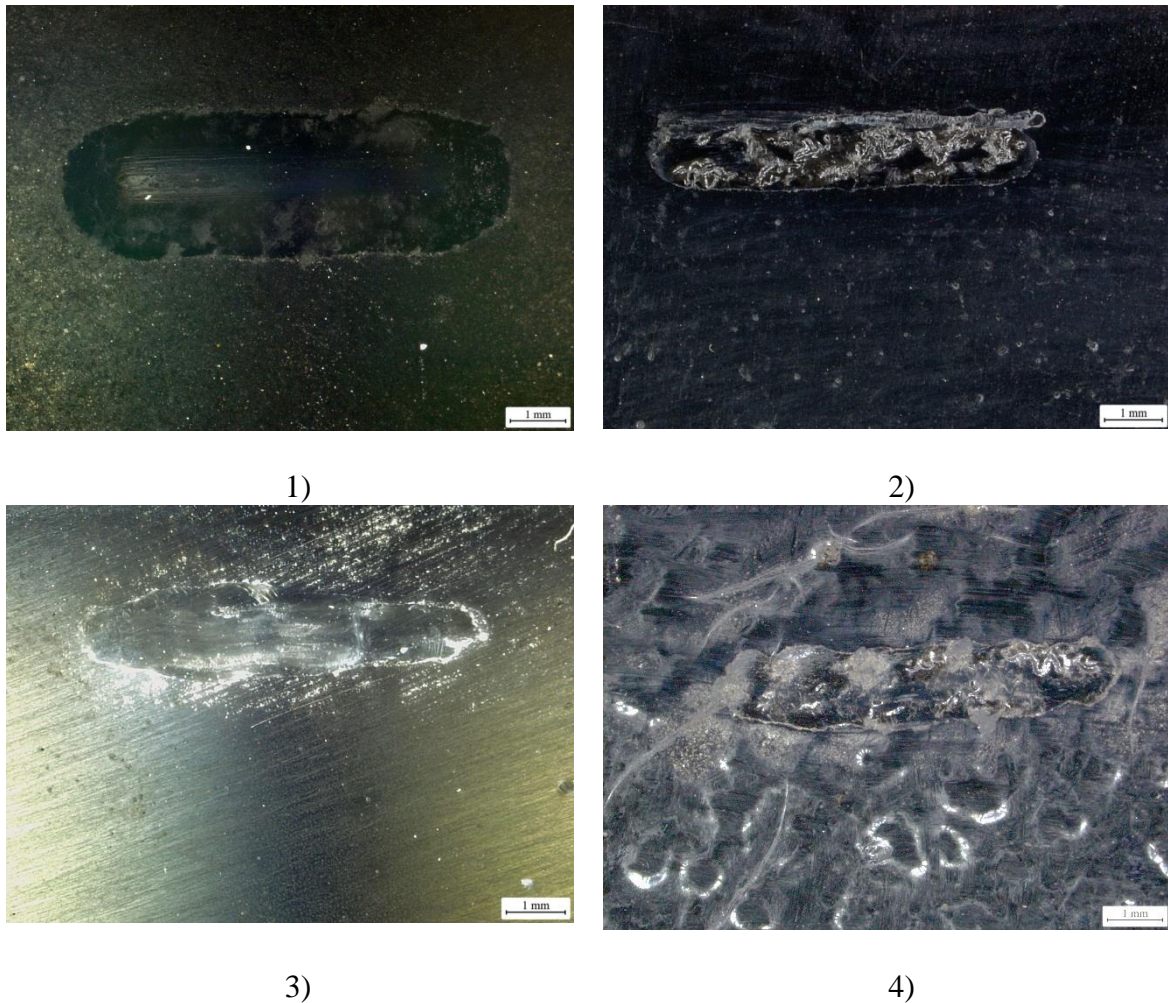


Fig. 5. Morphology of coating abrasion marks:1- Na_2SiO_3 graphite composite coating;2- GO gel composite coating;3- Na_2SiO_3 coating;4- SKH51+GO gel composite coating.

The surface of the grinding groove was observed by super depth-of-field microscope. Coating wear is mainly abrasive wear and polishing, as shown in Fig.6. The maximum width of the abrasion marks is surveyed with the measurement function of the super depth-of-field microscope. The light source and depth of field of the microscope were adjusted to get a clear edge of the abrasion mark. When the abrasion marks were measured, 6 sets of data from the middle section were taken, which were used to calculate the average and standard deviation. In Fig. 7, the graphene oxide coating deposited on 45 steel has the smallest abrasion marks, with an average width of $1283 \mu\text{m}$, and its standard deviation of $43 \mu\text{m}$. GO gel coating on SKH51 layer has the second narrowest abrasion marks, with an average width of $1378 \mu\text{m}$ and a standard deviation of $150 \mu\text{m}$. The average width of the abrasion marks on Na_2SiO_3 coating is $1416 \mu\text{m}$, with a variance of $234 \mu\text{m}$. In the Na_2SiO_3 graphite composite coating, the coating has the widest abrasion marks, and the layers have poor abrasion resistance, although the graphite has some lubricity. By comparison, it is shown that GO gel composite coatings have the best abrasion resistance. Graphene oxide particles are uniformly dispersed in the coating. Graphene oxide particles material can reduce the friction of the coating and increase the abrasion resistance.

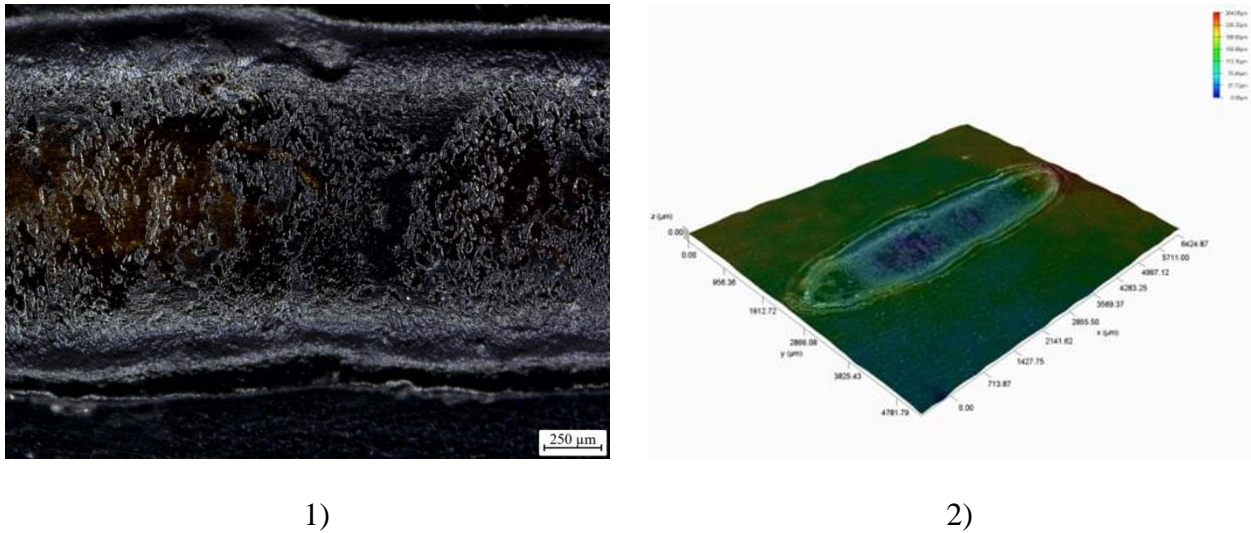


Fig. 6. Abrasive groove morphology:1-2D morphology;2-3D morphology;

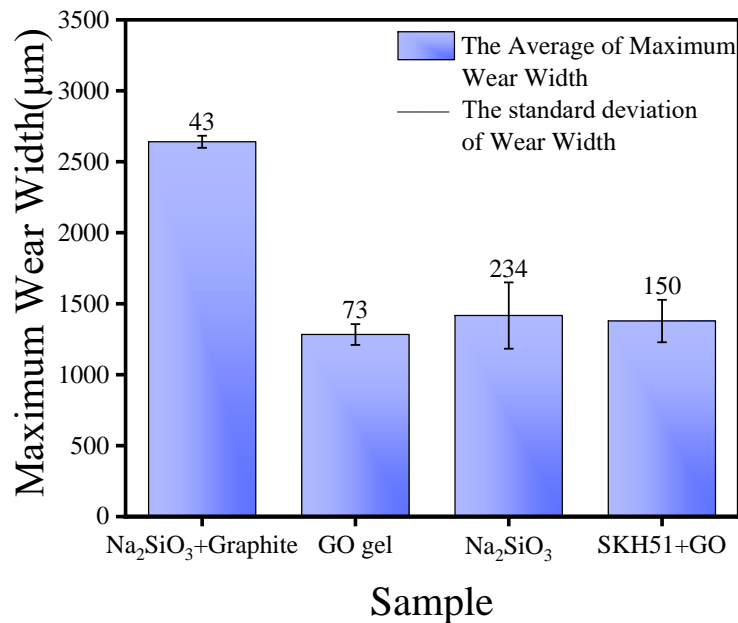


Fig. 7. Average and standard deviation of coating abrasion marks

7. Prospects for further research development

GO gel coating will be further investigated the effect of solidification temperature, solidification time, GO content and other factors on the coating. 1) This will lead to the optimal deposition process of GO gel coating. 2) The effect of the mixture of multiple wear-resistant particles and friction-reducing particles on the coating properties will be further studied to enhance the performance of ESD coatings.

8. Conclusions

GO gel coating can effectively improve the surface quality of the coating with less roughness. Graphene oxide belongs to nano-materials and can be uniformly dispersed in the coating. It can modify the ESD surface, reduce friction and increase wear resistance. It is an attempt to improve the surface accuracy of ESD coatings and reduce the processing cost.

1) The roughness quality of ESD coatings can be enhanced by Na_2SiO_3 coating and graphene oxide gel composite coating. The application of the GO gel composite coating onto the SKH51 surface resulted in a reduction of the roughness value from $1.086 \mu\text{m}$ to $0.113 \mu\text{m}$.

2) Graphene oxide gel is used to solve the problem of lubricating particle agglomeration. The friction coefficient of GO gel composite coating is 39.2% lower than that of Na_2SiO_3 coating. It can reduce the friction of non-metallic composite coatings and improve abrasion resistant. It can slow down the wear of ESD coatings.

3) The graphene oxide gel composite coating has the best wear resistance. Through research on the properties of graphene oxide gel, it was found that the friction coefficient was 0.17 and the grinding width was $1283.02 \mu\text{m}$. GO gel composite coating has the best overall performance.

References:

1) Compton, O. C., & Nguyen, S. T. J. s. (2010). Graphene oxide, highly reduced graphene oxide, and graphene: versatile building blocks for carbon-based materials. *6*(6), 711-723.

2) Ding, R., Li, W., Wang, X., Gui, T., Li, B., Han, P., . . . Compounds. (2018). A brief review of corrosion protective films and coatings based on graphene and graphene oxide. *764*, 1039-1055.

3) Dovzhik, M., Tarelnik, V., Marcinkovsky, V., & Pavlov, A. (2016). Restoring machine parts by electroerosive doping and applying polymer composites.

4) Enrique, P. D., Keshavarzkermani, A., Esmaeilzadeh, R., Peterkin, S., Jahed, H., Toyserkani, E., & Zhou, N. Y. J. A. M. (2020). Enhancing fatigue life of additive manufactured parts with electrospark deposition post-processing. *36*, 101526.

5) Gadalov, V., Romanenko, D., Samoilo, V., Nikolaenko, A., & Grigor'ev, S. J. R. J. o. N.-F. M. (2012). Procedure of evaluating the surface roughness of the electrospark coating after burnishing with mineral ceramics. *53*, 348-350.

6) Gao, Y., Fan, Y., Zhang, J., Liu, X., Wang, N., & Yang, S. J. M. (2021). The study of graphene oxide on the regulations and controls of the sol-gel film structure and its performance. *12*(1), 20.

7) Ghauri, F. A., Raza, M. A., Baig, M. S., & Ibrahim, S. J. M. R. E. (2017). Corrosion study of the graphene oxide and reduced graphene oxide-based epoxy coatings. *4*(12), 125601.

8) Huang, J., Zong, C., Shen, H., Cao, Y., Ren, B., & Zhang, Z. J. N. (2013). Tracking the intracellular drug release from graphene oxide using surface-enhanced Raman spectroscopy. *5*(21), 10591-10598.

9) Im, H., & Kim, J. J. C. (2012). Thermal conductivity of a graphene oxide-carbon nanotube hybrid/epoxy composite. *50*(15), 5429-5440.

10) Jiang, X., Dai, Y., Xiang, Q., Liu, J., Yang, F., Zhang, D. J. S., & Technology, C. (2021). Microstructure and wear behavior of inductive nitriding layer in Ti-25Nb-3Zr-2Sn-3Mo alloys. *427*, 127835.

11) Kirik, G. V., Gaponova, O. P., Tarelnyk, V. B., Myslyvchenko, O. M., & Antoszewski, B. (2018). Quality Analysis of Aluminized Surface Layers Produced by Electrospark Deposition. *Powder Metallurgy and Metal Ceramics*, *56*(11), 688-696. doi:10.1007/s11106-018-9944-6

12) Krishnamoorthy, K., Jeyasubramanian, K., Premanathan, M., Subbiah, G., Shin, H. S., & Kim, S. J. J. C. (2014). Graphene oxide nanopaint. *72*, 328-337.

13) Kumar, S. S. A., Bashir, S., Ramesh, K., & Ramesh, S. J. P. i. O. C. (2021). New perspectives on Graphene/Graphene oxide based polymer nanocomposites for corrosion applications: The relevance of the Graphene/Polymer barrier coatings. *154*, 106215.

14) Nakamizo, M., Kammereck, R., & Walker Jr, P. J. C. (1974). Laser Raman studies on carbons. *12*(3), 259-267.

15) Neklyudov, V. V., Khafizov, N. R., Sedov, I. A., & Dimiev, A. M. J. P. C. C. P. (2017). New insights into the solubility of graphene oxide in water and alcohols. *19*(26), 17000-17008.

16) Palmieri, V., Papi, M., Conti, C., Ciasca, G., Maulucci, G., & De Spirito, M. J. E. R. o. M. D. (2016). The future development of bacteria fighting medical devices: the role of graphene oxide. *13*(11), 1013-1019.

- 17) Ribalko, A. V., Sahin, O., & Korkmaz, K. (2009). A modified electrospark alloying method for low surface roughness. *Surface and Coatings Technology*, 203(23), 3509-3515. doi:<https://doi.org/10.1016/j.surfcoat.2009.05.002>
- 18) Shi, F., Zhang, Q., Xu, C., Hu, F., Yang, L., Zheng, B., . . . Technology, L. (2022). In-situ synthesis of NiCoCrMnFe high entropy alloy coating by laser cladding. *151*, 108020.
- 19) Smith, A. T., LaChance, A. M., Zeng, S., Liu, B., & Sun, L. J. N. M. S. (2019). Synthesis, properties, and applications of graphene oxide/reduced graphene oxide and their nanocomposites. *1(1)*, 31-47.
- 20) Sun, R., Chen, C., Ling, W.-J., Zhang, Y.-N., Kang, C.-P., & Xu, Q. (2019). Watt-level passively Q-switched mode-locked Tm: LuAG laser with graphene oxide saturable absorber. *Acta Physica Sinica*, 68(10), 104207-104201-104207-104206. doi:10.7498/aps.68.20182224
- 21) Tong, L., Zhang, J., Xu, C., Wang, X., Song, S., Jiang, Z., . . . Zhang, H. J. C. (2016). Enhanced corrosion and wear resistances by graphene oxide coating on the surface of Mg-Zn-Ca alloy. *109*, 340-351.
- 22) Wojtoniszak, M., Chen, X., Kalenczuk, R. J., Wajda, A., Łapczuk, J., Kurzewski, M., . . . Bionterfaces, S. B. (2012). Synthesis, dispersion, and cytocompatibility of graphene oxide and reduced graphene oxide. *89*, 79-85.
- 23) Yeh, C.-N., Raidongia, K., Shao, J., Yang, Q.-H., & Huang, J. J. N. c. (2015). On the origin of the stability of graphene oxide membranes in water. *7(2)*, 166-170.
- 24) Yu, W., Sisi, L., Haiyan, Y., & Jie, L. J. R. a. (2020). Progress in the functional modification of graphene/graphene oxide: A review. *10(26)*, 15328-15345.
- 25) Zhu, Y., Murali, S., Cai, W., Li, X., Suk, J. W., Potts, J. R., & Ruoff, R. S. J. A. m. (2010). Graphene and graphene oxide: synthesis, properties, and applications. *22(35)*, 3906-3924.